Some Outstanding Problems in Liquid Crystal Physics

Amit Kumar Bhattacharjee

Asutosh College, Kolkata

April 21, 2022

Organization

1. Background of nematic mesophases; statics and kinetics.
2. Numerical techniques and benchmarks.
3. Biaxiality of the isotropic-nematic interface; effect of rotational anchoring.
4. Shape of nematic bubble in isotropic background.
5. Phase ordering through spinodal kinetics.
6. Ongoing work.
7. Publications.

Background of Nematogens

- Anisotropic molecules (rods,discs) having long range orientational order devoid of translational order.
- Rotational symmetry about the direction of order, *uniaxial* phase $(\mathbf{n} \leftrightarrow -\mathbf{n})$.
- No rotational symmetry : *biaxial* order$(\mathbf{n} \leftrightarrow -\mathbf{n}, \mathbf{l} \leftrightarrow -\mathbf{l})$.
- Alignment tensor order have five degrees of freedom, 2 degrees of order and 3 angles to specify principal direction.
- $Q_{ij} = \frac{3}{2}S(n_i n_j - \frac{1}{3}\delta_{ij}) + \frac{T}{2}(l_i l_j - m_i m_j)(i, j = x, y, z)$.

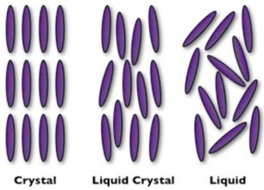

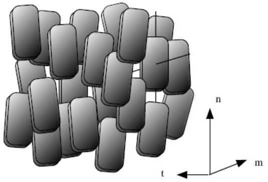

Statics : Free energy, phase diagram

$$\mathcal{F}[\mathbf{Q},\nabla\mathbf{Q}] = \int d^3\mathbf{x}[\frac{1}{2}ATr\mathbf{Q}^2 + \frac{1}{3}BTr\mathbf{Q}^3 + \frac{1}{4}C(Tr\mathbf{Q}^2)^2 + E'(Tr\mathbf{Q}^3)^2 + \frac{1}{2}L_1(\partial_\alpha Q_{\beta\gamma})(\partial_\alpha Q_{\beta\gamma}) + \frac{1}{2}L_2(\partial_\alpha Q_{\alpha\beta})(\partial_\gamma Q_{\beta\gamma})].$$

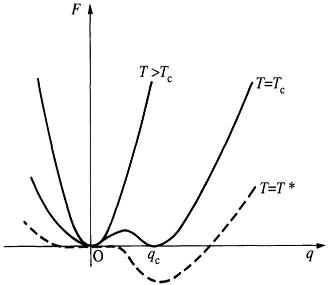

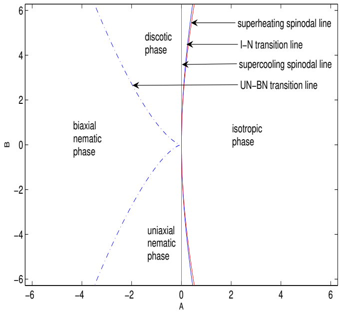

Kinetics

- Landau-Ginzburg model-A dynamics for non-conserved order parameter.
- $\partial_t Q_{\alpha\beta}(\mathbf{x},t) = -\Gamma_{\alpha\beta\mu\nu}\frac{\delta \mathcal{F}}{\delta Q_{\mu\nu}}$, where $\Gamma_{\alpha\beta\mu\nu} = \Gamma[\delta_{\alpha\mu}\delta_{\beta\nu} + \delta_{\alpha\nu}\delta_{\beta\mu} - \frac{2}{d}\delta_{\alpha\beta}\delta_{\mu\nu}]$.

$$\partial_t Q_{\alpha\beta}(\mathbf{x},t) = -\Gamma\ [(A + CTrQ^2)Q_{\alpha\beta}(\mathbf{x},t) + (B + 6E'TrQ^3)\ \overline{Q^2_{\alpha\beta}(\mathbf{x},t)}\ - L_1\nabla^2 Q_{\alpha\beta}(\mathbf{x},t) - L_2\ \overline{\nabla_\alpha(\nabla_\gamma Q_{\beta\gamma}(\mathbf{x},t))}\ ]$$

- Route to equilibrium $\Rightarrow$ nucleation kinetics above T^*, spinodal kinetics beneath T^*.
- $Q_{\alpha\beta}(\mathbf{x},t) = \sum_{i=1}^{5} a_i(\mathbf{x},t) T^i_{\alpha\beta}$, $\mathbf{T}^1 = \sqrt{\frac{3}{2}}\ \overline{\mathbf{z}\ \mathbf{z}}\ , \mathbf{T}^2 = \sqrt{\frac{1}{2}}(\mathbf{x}\ \mathbf{x} - \mathbf{y}\ \mathbf{y}), \mathbf{T}^3 = \sqrt{2}\ \overline{\mathbf{x}\ \mathbf{y}}\ , \mathbf{T}^4 = \sqrt{2}\ \overline{\mathbf{x}\ \mathbf{z}}\ ,$ $\mathbf{T}^5 = \sqrt{2}\ \overline{\mathbf{y}\ \mathbf{z}}\ .$

Problems at a glance

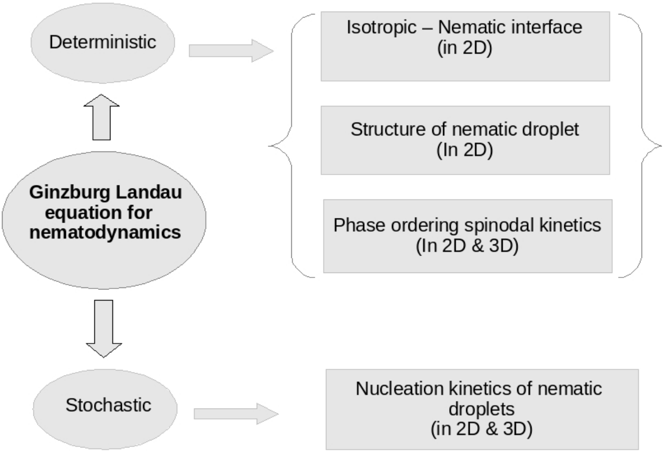

Numerical techniques

- Method of lines
  - Spatial finite difference discretization.
  - Temporal integration using standard library.
  - Benchmark of *tanh* interface, ellipsoidal droplet, corsening.
  - Performed in 2D on lattices, ranging from 256^2 to 1024^2.
  - Performed in 3D on lattices, ranging from 64^3 to 256^3.
- Spectral methods
  - Space discretized on chebyshev grids $x_j = cos(\pi j/N)$.
  - Global interpolation retaining the spectral accuracy.
- High-performance computation
  - Domain decomposition of the differentiation matrix and vector on a parallel cluster using standard library.
  - Structured binary data storage using standard library.

Isotropic-Nematic interface

- Verification of "de Gennes ansatz" and limitations using method of lines.
- Biaxial nature of IN interface with planar anchoring using spectral method.

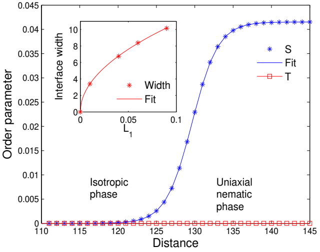

(a) $\kappa = 0$

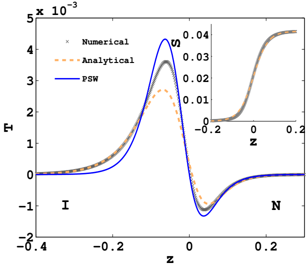

(b) $\kappa = 18$

Contd..

- Director anchoring at the interface with tilted anchoring at boundary.

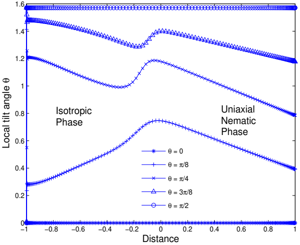

(c) $\kappa = 36$

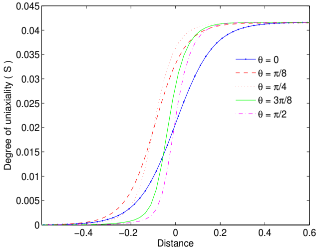

(d) $\kappa = 36$

Nematic droplet in isotropic background

- Nematic bubble grow or shrink in the nucleation regime.
- Contribution from the anisotropic surface tension $\Rightarrow$ shape change from circular to ellipsoidal.
- No approximation of surface free energy which automatically included in our formulation.
- Consequences : nucleation rate ($\propto e^{-B/k_B T}$) can be calculated exactly, apart from the prefactors.

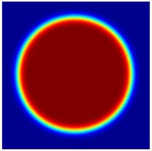

(e) $L_2 = 0$

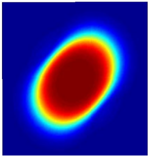

(f) $L_2 = 10L_1$

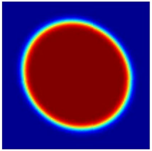

(g) $L_2 = -L_1$

Phase ordering kinetics

2D

1. Visualization and topological classification of point defects.
2. Structure of defect core of different homotopy class.
3. Dynamical scaling exponent.

3D

1. Line defects in nematics; intercommutation of defect segments.
2. Director configuration around the segment.
3. Topological rigidity in biaxial nematics.

Phase ordering kinetics

2D

1. Visualization and topological classification of point defects.
2. Structure of defect core of different homotopy class.
3. Dynamical scaling exponent.

3D

1. Line defects in nematics; intercommutation of defect segments.
2. Director configuration around the segment.
3. Topological rigidity in biaxial nematics.

Phase ordering kinetics

2D

1. Visualization and topological classification of point defects.
2. Structure of defect core of different homotopy class.
3. Dynamical scaling exponent.

3D

1. Line defects in nematics; intercommutation of defect segments.
2. Director configuration around the segment.
3. Topological rigidity in biaxial nematics.

Defects in nematics

- uniaxial nematic defects are characterized through $\pi_1(\mathbb{S}^2/\mathbb{Z}_2) = \mathbb{Z}_2$, having unstable integer and stable half integer charged defects.
- biaxial nematic defects are characterized through $\pi_1(\mathbb{S}^3/\mathbb{D}_2) = \mathbb{Q}_8$, having a stable integer ($\bar{C}_0$ class, 2π rotation of director) and three half-integer (C_x, C_y, C_z, π rotation of director) charged defects.
- Defects are visualized and classified through scalar order (movie).
- Textures (intensity $\propto sin^2[2\theta]$) show a subset while all the half-integer defect locations are identified in $S(\mathbf{x}, t), T(\mathbf{x}, t)$.

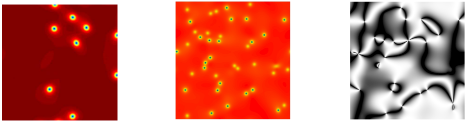

(h) (i) (j)

Core structure; dynamical scaling

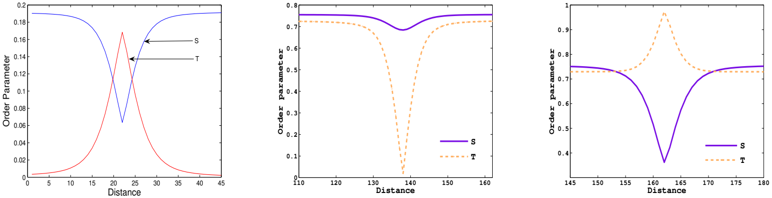

(k) (l) C_x (m) C_y

- Uniaxial dynamical scaling exponent $\alpha = 0.5 \pm 0.005$ $[L(t) \sim t^{\alpha}]$.

Line defects in 3D

- Point defects in 2D correspond to strings in 3D.
- Annihilation of point defect-antidefect correspond to formation and disappearance of loop.
- Line defects pass through each other through intercommutation i.e. exchanging segments (movie ; isosurface set to 0.054).
- Intercommutation of lines depend on the underlying abelian nature of the group elements of that particular homotopy group (Poenaru et.al. '77).
- No such signature seen in biaxial nematics !!

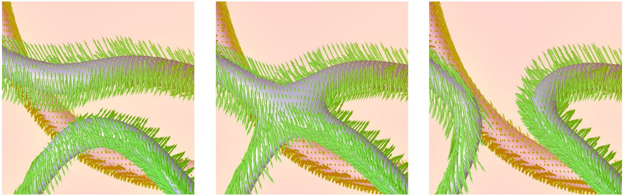

(n) (o) (p)

Ongoing work

- Nucleation kinetics in fluctuating nematics; nematic bubbles in 3D.
- Scaling exponent in 3D uniaxial and biaxial coarsening nematic (d=3,n=3).
- Scaling exponent of uniaxial nematic with space and spin dimension 2 (d=2,n=2).
- Topological rigidity in biaxial nematics ? Interplay of energetics over topology.

Publications

- Method of lines for the relaxational dynamics of nematic liquid crystals, PRE **78**, 026707 (2008).
- Biaxiality at the isotropic-nematic interface with planar anchoring, arXiv : 0906.2899 (submitted to PRE, Rapid Comm.).
- Simulation and visualization of disclinations in nematic liquid crystals (to be submitted in "Soft Matter").
- Nucleation kinetics in fluctuating Landau-de Gennes theory for uniaxial nematics (in preparation).
- Effect of general anchoring of the director on the isotropic-nematic interface (in preparation).

Thanks for your attention